Disorders of the Nervous System

Upregulation of nAChRs and Changes in Excitability on VTA Dopamine and GABA Neurons Correlates to Changes in Nicotine-Reward-Related Behavior

Austin T. Akers, [ID]Skylar Y. Cooper, Zachary J. Baumgard, Gabriella P. Casinelli, Alicia J. Avelar, and [ID]Brandon J. Henderson

Department of Biomedical Sciences, Marshall University, Joan C Edwards School of Medicine, Huntington, WV 25703

Abstract

Previous reports indicate that nicotine reward is mediated through $\alpha4\beta2*$, $\alpha6\beta2*$, and $\alpha4\alpha6\beta2*$ nicotinic acetylcholine receptors (nAChRs; $*$ indicates that additional nAChR subunits may be present). Little is known about $\alpha4\alpha6\beta2*$ nAChR involvement in reward and reinforcement because of a lack of methods that allow the direct investigation of this particular nAChR subtype. Here, we use male and female mice that contain $\alpha4$-mCherry and $\alpha6$-GFP nAChR subunits to show that concentrations of nicotine sufficient to evoke reward-related behavior robustly upregulate $\alpha4*$ and $\alpha4\alpha6*$ nAChRs on midbrain dopamine (DA) and GABA neurons. Furthermore, the extent of $\alpha4\alpha6*$ nAChR upregulation on ventral tegmental area (VTA) DA neurons aligns with the magnitude of nicotine reward-related behavior. We also show that the upregulation of nAChRs is accompanied by a functional change in firing frequency of both DA and GABA neurons in the VTA that is directly linked to nicotine reward-related behavior.

Key words: excitability; nicotine; nicotinic receptor; reward; upregulation

---

Significance Statement

This study reveals novel aspects of nicotinic acetylcholine receptor upregulation in the ventral tegmental area (VTA) and how it is linked to nicotine reward-related behavior. Nicotine is well characterized to upregulate these receptors, but our work here highlights the role that $\alpha4*$ and $\alpha4\alpha6*$ nicotinic acetylcholine receptors (nAChRs) play in the short term, intermittent exposure to nicotine that is consistent with early exposure to tobacco and vaping products.

Introduction

The use of tobacco or nicotine-containing products remains the leading cause of preventable death. Each year, nearly 6 million people die worldwide because of tobacco-related health complications (World Health Organization, 2011). In the United States alone, $\sim$480,000 people die annually from tobacco products resulting in $75 billion in medical costs [National Center for Chronic Disease Prevention and Health Promotion (US) Office on Smoking and Health, 2014]. Nicotine, the primary addictive component of tobacco products, stimulates dopamine (DA) neurotransmission through the activation of nicotinic acetylcholine receptors (nAChRs). Several nAChR subtypes contribute to the multiple stages of nicotine addiction, but many reports highlight $\alpha4\beta2*$, $\alpha6\beta2\beta3$, and $\alpha4\alpha6\beta2*$ nAChRs as primary mediators of nicotine reward, because these subtypes exhibit the highest sensitivity to acutely applied nicotine (Kuryatov and

Lindstrom, 2011; Liu et al., 2012; Engle et al., 2013). Furthermore, studies have shown that these nAChRs on VTA DA neurons are essential for intravenous self-administration of nicotine (Pons et al., 2008).

One well-studied phenomenon of $\alpha 4*$ (and in some cases $\alpha 6*$) nAChRs is that they upregulate following long-term exposure to nicotine (Marks et al., 1983; Nashmi et al., 2007; Jasinska et al., 2014; Henderson et al., 2016). These upregulated nAChRs exhibit an increase in sensitivity to nicotine (Kuryatov et al., 2005; Vallejo et al., 2005). In VTA DA neurons, $\alpha 4 \beta 2*$, $\alpha 6 \beta 2*$, and $\alpha 4 \alpha 6 \beta 2*$ nAChRs are upregulated by nicotine and the amount of upregulation depends on the concentration of nicotine used (Nashmi et al., 2007; Henderson et al., 2017). In ventral tegmental area (VTA) and substantia nigra pars reticulata (SNr) GABA neurons, $\alpha 4 \beta 2$ nAChRs are upregulated more robustly than nAChRs present on VTA DA neurons (Nashmi et al., 2007). The upregulated $\alpha 4 \beta 2$ nAChRs on GABA neurons exhibit increased sensitivity to nicotine reward (Nashmi et al., 2007; Ngolab et al., 2015) and are rapidly desensitized during acute nicotine exposure (Mansvelder et al., 2002), resulting in the disinhibition of VTA DA neurons and an increase in DA neurotransmission within the mesolimbic pathway. While the inhibitory inputs to VTA DA neurons are altered by nicotine, there is also an enhancement in excitatory inputs from medial VTA glutamate neurons (Yan et al., 2018, 2019). Together, these changes in inhibitory and excitatory transmission contribute to nicotine reward.

Despite general agreement that long-term nicotine exposure produces nAChR upregulation, there is little understanding regarding how nAChR upregulation is related to behaviors associated with nicotine reward or reinforcement. We sought to fill this gap in knowledge by assessing the magnitude of nAChR upregulation in mice that completed conditioned place preference (CPP) assays with nicotine. To accomplish this we used a previously characterized mouse line that contain $\alpha 4$-mCherry and $\alpha 6$-GFP nAChR subunits (Henderson et al., 2017). In using the same mice for both CPP and nAChR upregulation assays, we were able to establish direct links between nicotine reward-related behavior and nAChR upregulation.

Materials and Methods

Reagents
(–)-Nicotine dihydrogen ditartrate (product number AC415660100) was obtained from ACROS Organics. All doses and concentrations of nicotine listed here are given as free base.

Mice
All experiments were conducted in accordance with the guidelines for care and use of animals provided by the National Institutes of Health, and protocols were approved by the Institutional Animal Care and Use Committee at Marshall University. Mice were kept on a standard 12/12 h light/dark cycle at 22°C and given food and water ad libitum. At day 21, tail biopsies were taken for genotyping analysis by PCR. Genotyping was outsourced to a commercial lab to detect the presence of fluorescence proteins (Transnetyx). For microscopy assays, only mice that were transgenic for $\alpha 6$-GFP and homozygous for $\alpha 4$-mCherry were used (see CPP assay methods below), with the exception of $\alpha 6$-GFP and $\alpha 4$-mCherry mice used for NFRET controls. For electrophysiology assays we used $\alpha 6$-GFP mice. All experiments used adult (three to five months old) mice. Both male and female mice were used and numbers of each are detailed below in the methods for specific experiments.

CPP assays
CPP assays were completed with a three-chamber spatial place-preference chamber (Harvard Apparatus, PanLab) (Fig. 2). Time in chambers was recorded by video motion tracking software (SMART 3.0). An unbiased protocol was used where nicotine was given in the white/gray chamber on "drug" days, and saline was given in the white/black chamber on saline days. For saline-control cohorts, saline injections were given on both sides. On day 1 of testing, mice were placed in the central chamber and allowed free access for 20 min. Mice that spent >65% of the test in one chamber were judged to show initial biases and were excluded from the experiment. On days 2–5, mice were trained using twice-daily sessions. In morning sessions, mice were given an intraperitoneal injection of drug (saline or 0.5 mg/kg nicotine) immediately before confinement in the drug-paired chamber for 20 min. In the afternoon session, mice were given an intraperitoneal injection of saline immediately before confinement in the saline-paired chamber for 20 min. On day 6, a post-test was completed where the mice were again placed in the central chamber and allowed free access for 20 min. A total of 25 mice were used in CPP assays, and two were excluded because of initial bias. Nearly equal numbers of male and female mice, three to six months old, were used in CPP assays. No sex differences were observed at this dose of nicotine. Data are expressed as a change in baseline preference between the pre-test and post-test. Of these mice, 12 were later studied in confocal microscopy assays (see below).

Between the A.M. and P.M. CPP sessions, each mouse experienced a break of ~4 h. Given the pharmacokinetics of nicotine, injections up to 1 mg/kg are cleared in ≤1 h and most likely within 30 min (Matta et al., 2007; Li et al., 2013). Thus, nicotine is not present in the brain or plasma during the PM CPP saline conditioning sessions. For each cohort, only mice of the same sex were tested. All drugs used in CPP assays were dissolved in saline at pH 7.4 and injected intraperitoneally.

Confocal imaging of mouse brain slices

Some mice studied in CPP assays were also studied in microscopy assays. Drug delivery for these cohorts is described in the above CPP section. Following the completion of CPP assays, mice were euthanized with CO_2 and subjected to a quick cardiac perfusion with 10-ml ice-cold saline. We found that this significantly reduced the autofluorescence in the mCherry emission range. The brain was then quickly removed and frozen using acetone and dry ice and then stored at $-80°C$ overnight. At least 24 h later, brains were sectioned at $20\,\mu m$ using a cryostat onto glass slides (1.0 mm). Coronal brain slices were mounted with Vectashield (Vector Labs, H-1000) and coverslipped (1.5-mm thickness, glass). We targeted bregma -3.1 mm because this region gave the most consistent sections that contained a large portion of the VTA, SNr, substantia nigra pars compacta (SNc), and dentate gyrus in a single slice. In each session, brain slices from mice that received different drug treatments were selected according to bregma (-3.1 mm) so that all imaging sessions were matched between animals and across cohorts.

A Leica SP5 TCSII confocal microscope was used for imaging of the $\alpha4$-mCherry$\alpha6$-GFP mouse brain slices. $\alpha6$-GFP and $\alpha4$-mCherry were excited at 488 and 561 nm, respectively; $40\times$ images with a $5\times$ digital zoom were collected for the quantitative measurements of $\alpha4$-mCherry and $\alpha6$-GFP neuron raw integrated density (RID) of the midbrain, while $10\times$ images with a $5\times$ digital zoom were collected for the quantitative measurements of $\alpha4$-mCherry expression of the dentate gyrus. NFRET was calculated using the PixFRET ImageJ plug-in. Control data for NFRET donor and acceptor bleedthrough were obtained by imaging neurons from homozygous $\alpha4$-mCherry mice (wild-type $\alpha6$) and $\alpha6$-GFP (wild-type $\alpha4$) mice separately. In total, 19 male and 13 female mice were used in confocal assays following CPP (excluding those used for NFRET controls). Nearly equal numbers of male and female mice, three to five months old, were used and no sex differences were observed.

All calculations and analysis of GFP and mCherry fluorescence were made using ImageJ. We used RID as a metric for upregulation to match similar work on nAChR upregulation (Avelar et al., 2019; Cooper et al., 2020). For each mouse, two to three different brain slices were imaged by two to three experimenters blind to drug treatment until all data analysis was completed. For each brain slice, 41–71 VTA DA neurons, 36–50 VTA GABA neurons, or 36–68 SNr GABA neurons were imaged. Data were averaged to provide RID values for each mouse. To minimize biasing, we did not select subpopulations in each brain region and analyzed every GFP and/or mCherry neuron present in each brain area.

Calculation of upregulation score

Following microscopy assays of saline-treated and nicotine-treated mice from CPP assays, we calculated the mean RID for $\alpha4*$ ($\alpha4$-mCherry), $\alpha6*$ ($\alpha6$-GFP), and $\alpha4\alpha6*$ (identified by NFRET) nAChRs in saline-treated mice ($n = 6$ mice). We subtracted these mean RID values from the RID of individual mice used in the nicotine CPP cohort to obtain the upregulation score. For example, the upregulation scores for a hypothetical mouse X are calculated as following:

$$\alpha4mCherry_{UpregScore}^{MouseX} = \alpha4mCherry_{NicotineTreatedRID}^{MouseX} - MEAN\alpha4mCherry_{SalineTreatedRID}^{Mice1-6}$$

$$\alpha6GFP_{UpregScore}^{MouseX} = \alpha6GFP_{NicotineTreatedRID}^{MouseX} - MEAN\alpha6GFP_{SalineTreatedRID}^{Mice1-6}$$

$$\alpha4\alpha6_{UpregScore}^{MouseX} = \alpha4\alpha6_{NicotineTreatedRID}^{MouseX} - MEAN\alpha4\alpha6_{SalineTreatedRID}^{Mice1-6}.$$

These upregulation scores are plotted as y-axis values with the mouse's respective CPP scores as the x-axis values (see Figs. 3, 4). For linear regression analysis, we used GraphPad Prism software with no constraints on the data. This analysis in GraphPad provided R^2, F, and p values.

Immunofluorescence

For immunofluorescence assays (Fig. 1 only), we used three-month-old $\alpha6$-GFP mice. Mice were anesthetized in a manner identical to the method used for microscopy. However, before brain extraction, mice were perfused with 20-ml PBS and 40 ml 4% paraformaldehyde. Brains were extracted and placed in 40% sucrose for 24 h. Brains were sliced at a thickness of $20\,\mu m$ and mounted on microscope slides. Brain sections on slides were rinsed twice for 10 min with PBS and then permeabilized with 0.5% Triton X-100 in PBS for 1 h. Brain sections were then blocked with 4% goat serum in PBS for 45 min. The primary antibody was diluted in 4% goat serum in PBS and incubated overnight at 24°C [rabbit anti-GFP (A11122, Invitrogen) and sheep anti-TH (AB1542, Millipore) both at concentrations of 1:500]. Brain sections were then washed three times for 15 min with PBS, and the secondary antibody was diluted in 4% goat serum in PBS and incubated for 1 h at 24°C [goat anti-rabbit Alexa Fluor 488 (A11008, Invitrogen) and donkey anti-sheep Alexa Fluor 647 (ab150179, Abcam) both at concentrations of 1:1000]. Brain sections were washed three times for 15 min with PBS and mounted with Vectashield. Finally, brain slices were imaged using the same confocal microscope used for direct imaging of $\alpha4$-mCherry$\alpha6$-GFP mouse brain slices as described above.

Whole-cell patch-clamp electrophysiology

Recordings were performed using brain slices prepared from three-month-old male $\alpha6$-GFP mice. We used $\alpha6$-GFP mice because $\alpha6$ nAChR subunits are selectively expressed in DA neurons in the lateral VTA ($_L$VTA) and SNc and provide a method to identify putative DA (pDA) neurons (see Fig. 1). Previous investigations have also concluded that $\alpha6$-GFP expression in the $_L$VTA and SNc completely overlaps with the expression of tyrosine hydroxylase (TH; Mackey et al., 2012). To match the
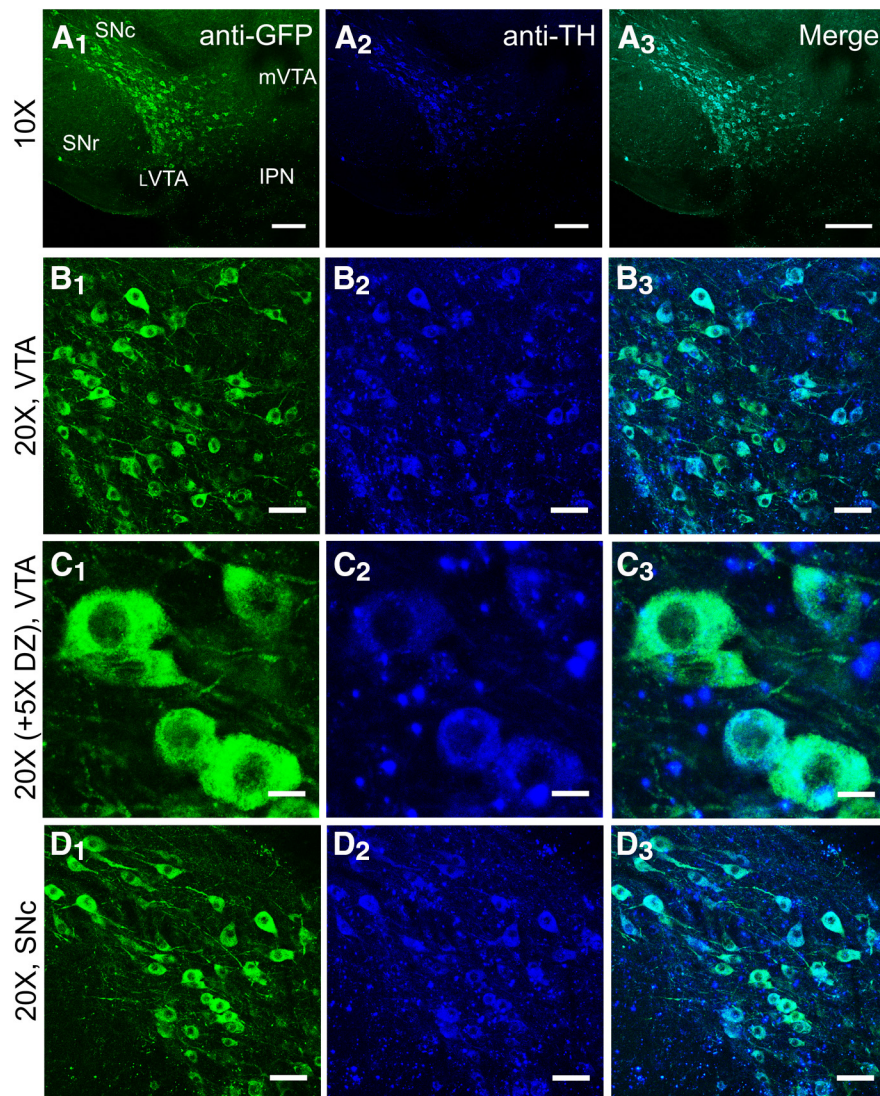
Figure 1. Presence of α6-GFP overlaps with presence of TH. A_1–A_3, 10× images of an α6-GFP mouse coronal brain slice (bregma, −3.1) immunostained with anti-GFP/Alexa Fluor 488 and anti-TH/Alexa Fluor 647. B, 20× image of neurons in the LVTA displaying overlap of α6-GFP and TH presence. C, 20× (with 5× digital zoom) images of LVTA. D, 20× Images of SNc neurons. Scale bars: 100 μm (A_1–A_3), 50 μm (B_1–B_3, D_1–D_3), and 10 μm (C_1–C_3).
Figure Contributions: Brandon J. Henderson performed the experiments.

investigation of VTA DA neurons in microscopy assays, we targeted bregma −3.1 for electrophysiology assays. Mice were anesthetized with CO_2 and were subjected to cardiac perfusion. The artificial cerebral spinal fluid solutions we used were made in accordance to the protective recovery method (www.brainslicemethods.com). We used standard artificial CSF (ACSF; containing the following: 125 mM NaCl, 2.5 mM KCl, 1.2 mM NaH_2PO_4, 1.2 mM $MgCl_2$, 2.4 mM $CaCl_2$, 26 mM $NaHCO_3$, and 11 mM glucose, adjusted to 300–310 mOsm and pH 7.4) for transcardial perfusion and brain slicing (250-μm coronal sections). Following cutting, brain slices containing VTA DA neurons were allowed to recover at 32–34°C in a NMDG ACSF solution (containing the following: 93 mM NMDG, 2.5 mM KCl, 1.2 mM NaH_2PO_4, 30 mM $NaHCO_3$, 20 mM HEPES, 25 mM glucose, 5 mM Na-ascorbate, 2 mM

thiourea, 3 mM Na-pyruvate, 10 mM $MgSO_4$, and 0.5 mM $CaCl_2$, adjusted to 300–310 mOsm and pH 7.4) for 15 min. Next, brain slices remained in standard ACSF at room temperature for ≥60 min. Slices were then transferred to the slice chamber and continually perfused with carbogen-saturated standard ACSF (1.5–2.0 ml/min) at 32°C.

Neurons were visualized with an upright microscope (Axio Examiner A1, Zeiss) equipped with an Axiocam 702 mono using DIC near-infrared illumination. Blue illumination was used to visualize α6-GFP presence in pDA neurons. Cell-attached and whole-cell patch-clamp techniques were used to record electrophysiological signals with an Integrated Patch-Clamp Amplifier (Sutter). Patch electrodes had resistances of 4–10 MΩ when filled with intrapipette solution: 135 mM K gluconate, 5 mM KCl, 5 mM EGTA, 0.5 mM $CaCl_2$, 10 mM HEPES, 2 mM Mg-ATP, and 0.1 mM GTP (adjusted to

280–300 mOsm and pH of 7.4). Recordings were sampled at 10–40 kHz. The junction potential between patch pipette and bath solutions was nulled just before gigaseal formation. Series resistance was monitored without compensation throughout experiments using SutterPatch software. The recording sessions for neurons were terminated if the series resistance changed by >20%. Nicotine (hydrogen tartrate salt, dissolved in standard ACSF at pH 7.4) applications were applied using a Picospritzer III (Parker) at a pressure of 5 psi for 20 s at concentration of 300 and 500 μM.

Statistical analysis

All results are presented as mean ± SEM, and all statistical analyses were performed using GraphPad Prism. For CPP assays, upregulation, and comparison of firing frequencies, we used an unpaired, two-tailed t test to compare saline-treated and nicotine-treated groups. For correlations between CPP scores and nAChR upregulation, we used GraphPad Prism software to perform linear regression analysis. All statistical test results are presented in Table 1.

Results

Nicotine reward-related behavior in α4-mCherryα6-GFP mice

Given that our goal was to investigate a link between nAChR upregulation and nicotine reward-related behavior, we required a method to reliably identify DA and GABA neurons in the VTA. To distinguish between DA and GABA neurons in the VTA, we used the presence of α6-GFP nAChRs in a manner that is similar to previous reports that have used fluorescently tagged nAChR subunits (Henderson et al., 2014, 2016, 2017; Cooper et al., 2020). Previous investigations have shown that α6-GFP or β3-GFP nAChRs that are selectively expressed in VTA and SNc DA neurons exhibit a high co-localization with TH presence (>95%; Mackey et al., 2012; Srinivasan et al., 2016). To confirm this using our own methods, we used immunofluorescence on coronal brain slices (bregma, −3.1) from α4-mCherryα6-GFP mice to examine the co-localization of α6-GFP in this mouse line with TH (Fig. 1). Here, we observed that 100% of the α6-GFP-labeled neurons in the $_L$VTA and SNc co-localized with TH (Fig. 1; Table 2). Conversely, 83.9% and 73.9% of the TH-positive neurons contained α6-GFP in the $_L$VTA and SNc, respectively (Fig. 1; Table 2). We acknowledge that α6 nAChR subunits are expressed on GABAergic boutons in the VTA (Yang et al., 2011). Accordingly, we have assigned neurons positive for α6-GFP expression as pDA neurons.

The α4-mCherryα6-GFP mice enable the examination of α4β2∗, α6β2∗, and α4α6β2∗ nAChRs in midbrain DA and GABA neurons (Fig. 2A,B; Henderson et al., 2017). We tested mice using a CPP assay to measure reward-related behavior (Fig. 2C). In rodents, acute nicotine produces rewarding effects depending on route of administration and concentration. Previous investigations have reported that mice exhibit reward-related

behavior to 0.5 mg/kg nicotine in a CPP assay (Tapper et al., 2004; Sanjakdar et al., 2015; Henderson et al., 2016, 2017). In agreement with these previous reports, male and female α4-mCherryα6-GFP mice exhibited significant reward-related behavior to intraperitoneal injections of 0.5 mg/kg nicotine when compared with saline ($p = 0.0011$ and $p = 0.006$, respectively; Fig. 2C). No sex differences were noted with this single dose of nicotine (Table 1), but we acknowledge this may not be the case if the dose range were to be expanded.

Our CPP experiments used intraperitoneal injections of 0.5 mg/kg nicotine. Based on nicotine pharmacokinetics in mice (Matta et al., 2007), these daily injections produced a "peak" brain concentration of ∼250 nM nicotine that would be eliminated in ∼30 min. This would be applicable to beginning smokers in the early stages of dependence (Tapper et al., 2004). It is important to note that nAChRs on VTA DA neurons would be functionally activated at this concentration of nicotine as previous investigations show that 300 nM nicotine is sufficient to evoke inward currents in VTA DA neurons (Liu et al., 2012; Engle et al., 2013). These previous reports also stress that this low concentration of nicotine only activates nAChRs that contain both α4 and α6 nAChR subunits. To confirm this, we conducted our own whole-cell patch-clamp electrophysiology assays to determine whether 300 and 500 nM nicotine stimulates inward currents in VTA DA neurons. We prepared brain slices from three-month-old male α6-GFP mice (target bregma, −3.1). VTA pDA neurons were identified by presence of α6-GFP (Fig. 2E1), firing frequencies <10 Hz, and presence of I$_h$ (Margolis et al., 2006). pDA neurons were voltage clamped at −65 mV, and 300 or 500 nM nicotine was puffed onto target neurons for 10 s (Fig. 2E2,E3). We noted inward currents in 80% of pDA neurons to both concentrations of nicotine, similar to previous reports (Liu et al., 2012; Engle et al., 2013). This suggests that the concentrations of nicotine used in our CPP assays not only produced reward-related behavior but also were sufficient to activate nAChRs on VTA pDA neurons.

Upregulation of α4α6∗, α4∗, and α6∗ nAChRs in VTA DA neurons

To determine whether nAChR upregulation correlates to nicotine reward-related behavior, we used confocal microscopy assays similar to previous investigations into nAChR upregulation (Henderson et al., 2014, 2016, 2017). Coronal mouse brain slices containing the VTA, SNc, and SNr (bregma, −3.1) were prepared from mice subjected to the CPP assay (Fig. 2A,C).

As discussed above, we used the presence of α6-GFP to distinguish between DA and GABA neurons in the VTA for our assays using inherent fluorescence (no immunostaining; Fig. 2A,B). Using FRET methods that have been described previously (Henderson et al., 2017; Avelar et al., 2019), we identified regions of neurons that contain α4α6β2∗ nAChRs. Upregulation of nAChRs was assessed by quantifying the change in RID of α6-GFP or α4-mCherry fluorescence. We observed a significant increase in the RID of α4α6∗ nAChRs in VTA

Table 1: Stats table

Figure	Figure panel	Statistical test	Conditions	Results
2	C	Two-way ANOVA interaction		$F_{(1,35)} = 0.016$ $p = 0.90$
		Two-way ANOVA sex factor		$F_{(1,35)} = 0.02$ $p = 0.89$
		Two-way ANOVA drug factor		$F_{(1,35)} = 23.9$ $p = 0.00002$
		Two-way ANOVA means comparison	Male mice (CPP, saline vs nicotine)	$p = 0.0011$
		Two-way ANOVA means comparison	Female mice (CPP, saline vs nicotine)	$p = 0.0064$
	D_1	Two-way ANOVA interaction	$\alpha4\alpha6*$ nAChR upregulation	$F_{(1,23)} = 0.45$ $p = 0.51$
		Two-way ANOVA sex factor	$\alpha4\alpha6*$ nAChR upregulation	$F_{(1,25)} = 0.12$ $p = 0.73$
		Two-way ANOVA drug factor	$\alpha4\alpha6*$ nAChR upregulation	$F_{(1,25)} = 19.0$ $p = 0.0002$
		Two-way ANOVA means comparison	Male mice ($\alpha4\alpha6*$ RID, saline vs nicotine)	$p = 0.019$
		Two-way ANOVA means comparison	Female mice ($\alpha4\alpha6*$ RID, saline vs nicotine)	$p = 0.0054$
	D_2	Two-way ANOVA interaction	$\alpha4*$ nAChR upregulation	$F_{(1,25)} = 0.74$ $p = 0.40$
		Two-way ANOVA sex factor	$\alpha4*$ nAChR upregulation	$F_{(1,25)} = 0.30$ $p = 0.59$
		Two-way ANOVA drug factor	$\alpha4*$ nAChR upregulation	$F_{(1,25)} = 15.5$ $p = 0.0005$
		Two-way ANOVA means comparison	Male mice ($\alpha4*$ RID, saline vs nicotine)	$p = 0.05$
		Two-way ANOVA means comparison	Female mice ($\alpha4*$ RID, saline vs nicotine)	$p = 0.008$
	D_3	Two-way ANOVA interaction	$\alpha6*$ nAChR upregulation	$F_{(1,25)} = 0.32$ $p = 0.58$
		Two-way ANOVA sex factor	$\alpha6*$ nAChR upregulation	$F_{(1,25)} = 0.87$ $p = 0.36$
		Two-way ANOVA drug factor	$\alpha6*$ nAChR upregulation	$F_{(1,25)} = 0.086$ $p = 0.77$
		Two-way ANOVA means comparison	Male mice ($\alpha6*$ RID, saline vs nicotine)	$p = 0.99$
		Two-way ANOVA means comparison	Female mice ($\alpha6*$ RID, saline vs nicotine)	$p = 0.99$
3	A_2	Linear regression	Male mice, CPP score vs VTA pDA $\alpha4\alpha6*$ nAChR upregulation	$R^2 = 0.67$ $F_{(1,5)} = 10.1$ $p = 0.025$
	A_3	Linear regression	Male mice, CPP score vs VTA pDA $\alpha4*$ nAChR upregulation	$R^2 = 0.83$ $F_{(1,5)} = 24.4$ $p = 0.004$
	A_4	Linear regression	Male mice, CPP score vs VTA pDA $\alpha6*$ nAChR upregulation	$R^2 = 0.74$ $F_{(1,5)} = 14.3$ $p = 0.013$
	B_1	Linear regression	Female mice, CPP score vs VTA pDA $\alpha4\alpha6*$ nAChR upregulation	$R^2 = 0.82$ $F_{(1,6)} = 28.2$ $p = 0.002$
	B_2	Linear regression	Female mice, CPP score vs VTA pDA $\alpha4*$ nAChR upregulation	$R^2 = 0.81$ $F_{(1,6)} = 25.6$ $p = 0.002$
	B_3	Linear regression	Female mice, CPP score vs VTA pDA $\alpha6*$ nAChR upregulation	$R^2 = 0.07$ $F_{(1,6)} = 0.47$ $p = 0.52$
	C_2	Linear regression	CPP score vs VTA pDA $\alpha4\alpha6*$ nAChR upregulation	$R^2 = 0.08$ $F_{(1,3)} = 0.24$ $p = 0.65$
	C_3	Linear regression	CPP score vs VTA pDA $\alpha4*$ nAChR upregulation	$R^2 = 0.08$ $F_{(1,3)} = 0.26$ $p = 0.64$
	C_4	Linear regression	CPP score vs VTA pDA $\alpha6*$ nAChR upregulation	$R^2 < 0.01$ $F_{(1,3)} = 0.01$ $p = 0.94$

(Continued)

Table 1: Continued

Figure	Figure panel	Statistical test	Conditions	Results
4	A_2	Two-way ANOVA interaction	$\alpha 4*$ nAChR upregulation	$F_{(1,27)} = 0.99$ $p = 0.33$
		Two-way ANOVA sex factor	$\alpha 4*$ nAChR upregulation	$F_{(1,27)} = 2.86$ $p = 0.10$
		Two-way ANOVA drug factor	$\alpha 4*$ nAChR upregulation	$F_{(1,27)} = 17.1$ $p = 0.0003$
		Two-way ANOVA means comparison	Male mice ($\alpha 4*$ RID, saline vs nicotine)	$p = 0.0012$
		Two-way ANOVA means comparison	Female mice ($\alpha 4*$ RID, saline vs nicotine)	$p = 0.05$
	A_3	Linear regression	Male CPP score vs SNr GABA $\alpha 4*$ nAChR upregulation	$R^2 = 0.55$ $F_{(1,6)} = 7.39$ $p = 0.04$
	A_4	Linear regression	Female CPP score vs SNr GABA $\alpha 4*$ nAChR upregulation	$R^2 = 0.56$ $F_{(1,6)} = 6.45$ $p = 0.05$
	B_2	Two-way ANOVA interaction	$\alpha 4*$ nAChR upregulation	$F_{(1,24)} = 0.43$ $p = 0.52$
		Two-way ANOVA sex factor	$\alpha 4*$ nAChR upregulation	$F_{(1,24)} = 0.38$ $p = 0.55$
		Two-way ANOVA drug factor	$\alpha 4*$ nAChR upregulation	$F_{(1,24)} = 14.0$ $p = 0.001$
		Two-way ANOVA means comparison	Male mice ($\alpha 4*$ RID, saline vs nicotine)	$p = 0.04$
		Two-way ANOVA means comparison	Female mice ($\alpha 4*$ RID, saline vs nicotine)	$p = 0.013$
	B_3	Linear regression	Male CPP score vs SNr GABA $\alpha 4*$ nAChR upregulation	$R^2 < 0.001$ $F_{(1,6)} < 0.001$ $p = 0.99$
	B_4	Linear regression	Female CPP score vs SNr GABA $\alpha 4*$ nAChR upregulation	$R^2 = 0.075$ $F_{(1,6)} = 0.40$ $p = 0.55$
	D_1	Unpaired t test	Dentate Gyrus $\alpha 4*$ nAChR upregulation, saline vs nicotine	$p = 0.047$
	D_2	Linear regression	CPP score vs dentate gyrus $\alpha 4*$ nAChR upregulation	$R^2 = 0.02$ $F_{(1,4)} = 0.09$ $p = 0.78$
5	C	Unpaired t test	CPP score, saline vs nicotine	$p = 0.026$
	E	Unpaired t test	VTA pDA neuron firing frequency, saline vs nicotine	$p = 0.0094$
	F	Linear regression	CPP Score vs VTA pDA neuron firing frequency	$R^2 = 0.65$ $F_{(1,16)} = 11.2$ $p = 0.016$
6	D	Unpaired t test	VTA pGABA neuron firing frequency, saline vs nicotine	$p = 0.0056$
	E	Linear regression	CPP Score vs VTA pGABA neuron firing frequency	$R^2 = 0.77$ $F_{(1,16)} = 20.3$ $p = 0.004$

DA neurons of both male and female mice used to CPP assays ($p = 0.019$ and $p = 0.005$ for males and females, respectively; Fig. 2D1). We also noted a significant increase in $\alpha 4*$ nAChR RID in VTA pDA neurons ($p = 0.05$ and $p = 0.008$ for males and females, respectively; Fig. 2D2). This finding is similar to our previous study, which showed a non-significant increase in $\alpha 4*$ nAChR RID using alternating daily injections of 0.5 mg/kg nicotine and saline (Henderson et al., 2017). We observed no change in $\alpha 6$-GFP RID in VTA pDA neurons following nicotine treatment (Fig. 2D3). Similar to our CPP

Table 2: Immunofluorescence

	VTA	SNc
Number of TH+	768	184
Number of GFP+	644	136
% of GFP+ to TH+	83.9%	73.9%

All GFP+ neurons overlapped with TH+ neurons.

assays, we detected no differences between males and females (Table 1).

Upregulation of $\alpha 4 \alpha 6*$ and $\alpha 4*$ nAChRs in VTA pDA neurons correlates to nicotine reward-related behavior

Following the observations described above, we analyzed nAChR upregulation for individual mice as a function of their individual CPP score. For each mouse we calculated upregulation scores for $\alpha 4*$, $\alpha 6*$, and $\alpha 4 \alpha 6*$ nAChRs (defined in Materials and Methods), which we then plotted against the individual mouse's CPP score (Fig. 3A1–A4,B1–B3). We found that $\alpha 4 \alpha 6*$ nAChR upregulation in VTA pDA neurons significantly correlated to changes in nicotine reward-related behavior (CPP score) with a R^2 of 0.67 for males ($F_{(1,5)} = 10.1$, $p = 0.02$; Fig. 3A2) and a R^2 of 0.82 for females ($F_{(1,6)} = 28.2$, $p = 0.002$; Fig. 3B1). We also observed a
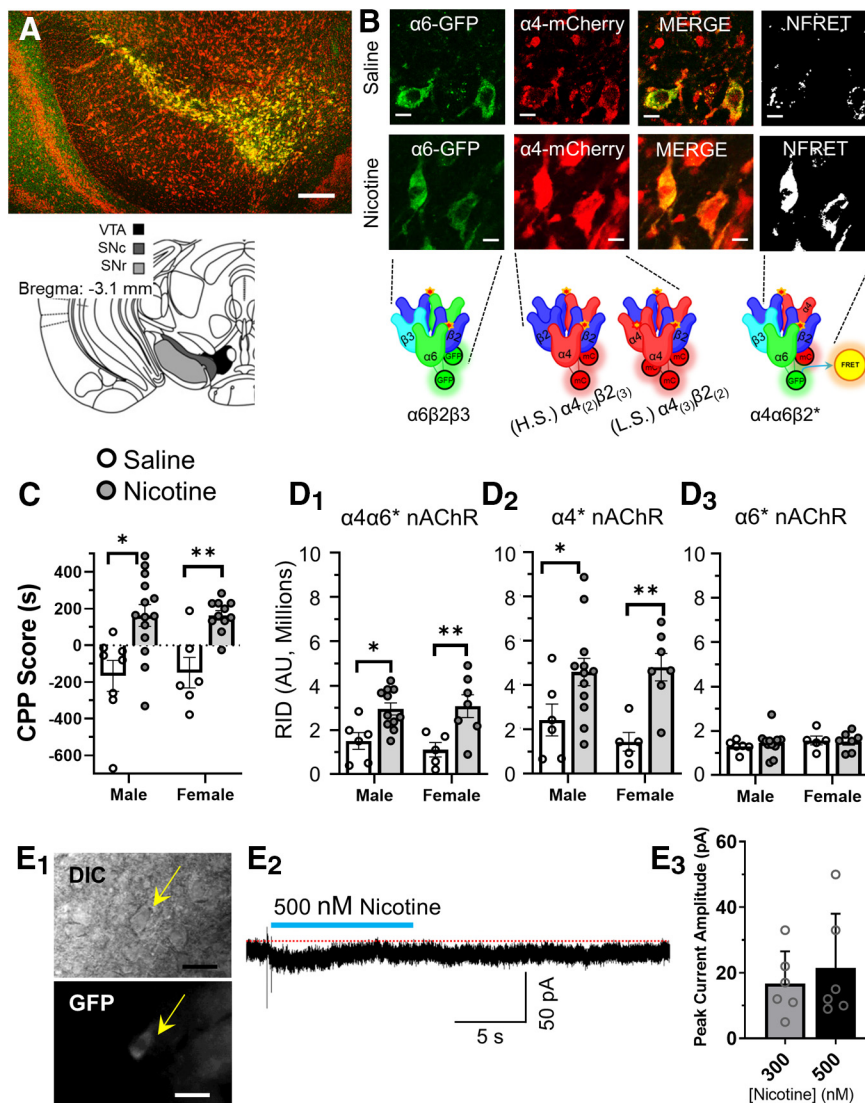
Figure 2. α4-mCherryα6-GFP mice reveal multiple subtypes of nAChRs on VTA pDA neurons. ***A***, Schematic of target mouse brain region (bottom) and sample 10$\times$ image of a mouse coronal brain slice at approximately bregma -3.1 mm (top, no immunofluorescence was used here). Scale bar: 250 μm. ***B***, Sample images of control and nicotine-treated VTA DA neurons, set to the same intensity scale, from α4-mCherryα6-GFP mice used in a CPP assay. Scale bar: 10 μm. ***C***, Male and female mice were administered intraperitoneal injections of saline or 0.5 mg/kg nicotine in a CPP assay [$n = 14$ (8 males and 6 females) and 25 (14 males and 11 females) for saline and nicotine, respectively]. ***D1–D3***, RID of α4α6*, α4*, and α6* nAChRs in saline-treated and nicotine-treated mice (from CPP assays). Individual dots represent the RID of individual mice [$n = 11$ (6 males and 5 females) and 19 (12 males and 7 females) for saline and nicotine, respectively]. For each mouse, 41–71 putative $_L$VTA DA neurons were imaged. ***E1***, Representative image of a putative VTA DA neuron in a brain slice (bregma, -3.1) from an α6-GFP mouse (scale bars: 20 μm). ***E2***, Representative voltage-clamp recording of putative $_L$VTA DA neurons during a 10-s puff of 300 and 500 n$_M$ nicotine. Blue bar indicates duration of nicotine puff and red dotted line represents baseline before nicotine puff. All data are mean $\pm$ SEM; *$p < 0.05$, **$p < 0.05$, ***$p < 0.005$; unpaired, two-tailed t test. Exact p values are given in Results.
Figure Contributions: Austin T. Akers, Zachary J. Baumgard, Skylar Y. Cooper, Gabriella P. Casinelli, Alicia J. Avelar, and Brandon J. Henderson performed the experiments and analyzed the data.

significant correlation between α4* nAChR upregulation in VTA pDA neurons and nicotine reward-related behavior. Here, we noted a R^2 of 0.83 ($F_{(1,5)} = 24.4$, $p = 0.004$; Fig. 3*A3*) in males and a R^2 of 0.81 ($F_{(1,6)} = 25.6$, $p = 0.002$; Fig. 3*B2*) in females. While we observed a significant correlation between α6* nAChR upregulation and nicotine reward-related behavior in male mice (R^2 of 0.74, $F_{(1,5)} = 14.3$, $p = 0.01$), we

note that four of the 6 data points are at the level of zero upregulation. We observed no correlation between α6* nAChR upregulation and reward-related behavior in female mice (Fig. 3*B3*). Using the same methodology, we examined upregulation of the nAChR subtypes in VTA DA neurons from the saline-treated group (Fig. 3*C1–C4*). Here, we found no correlation between changes in nAChR RID and reward-related
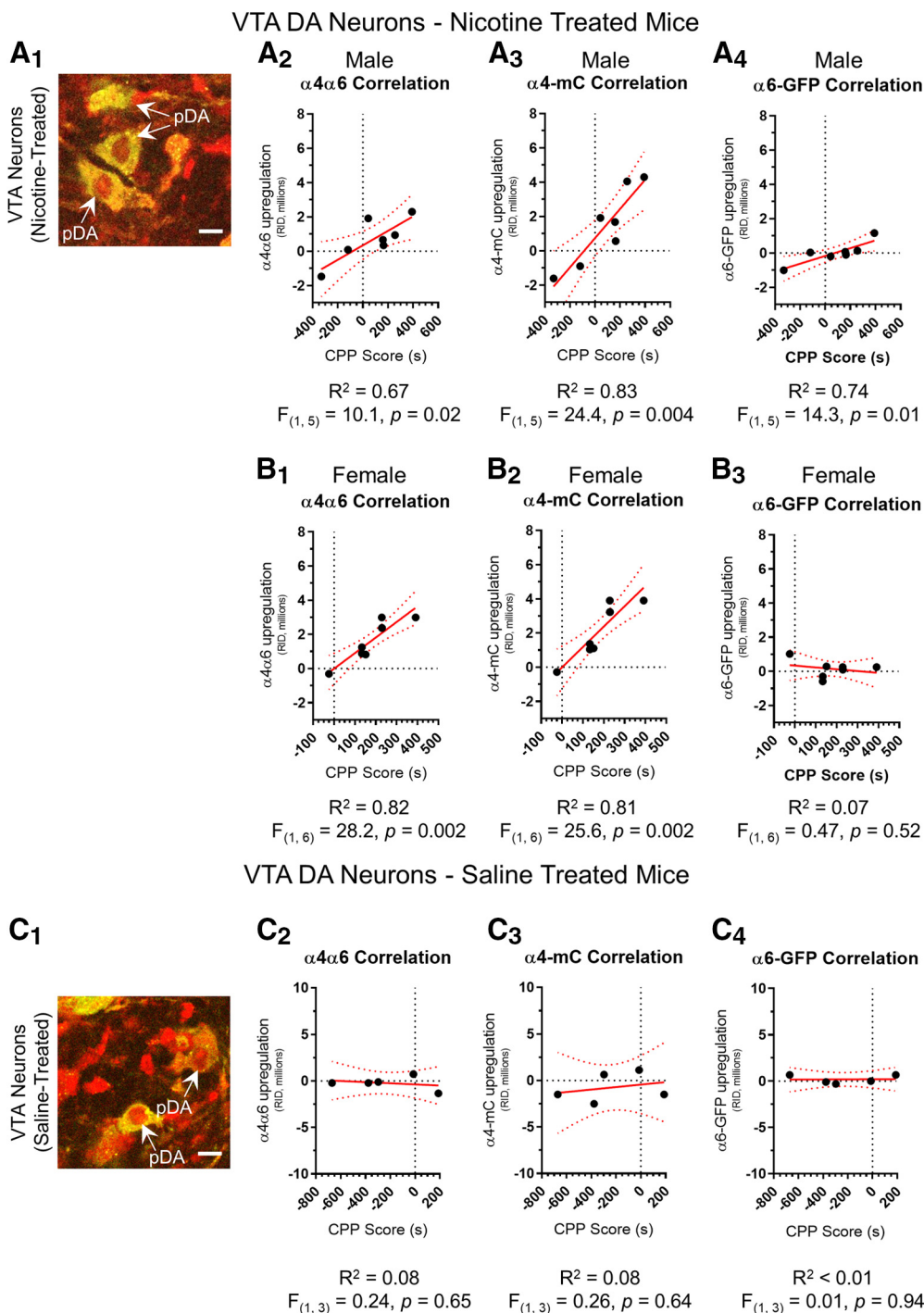
Figure 3. Upregulation of $\alpha4\alpha6*$ and $\alpha4*$ nAChRs in VTA pDA neurons correlates with nicotine reward-related behavior. A_1, C_1, Representative merged images of $_L$VTA DA neurons in a $\alpha4$-mCherry$\alpha6$-GFP brain slice. Scale bar, 10 μm. In nicotine-treated mice, changes in nAChR RID was correlated to CPP score for $\alpha4\alpha6*$ nAChRs, $\alpha4*$ nAChRs, and $\alpha6*$ nAChRs for male (A_2, A_3, A_4) and female (B_1, B_2, B_3) mice. Linear fits (red line) with 95% confidence intervals (dotted red lines). In saline-treated mice, changes in nAChR RID was correlated to CPP score for $\alpha4\alpha6*$ nAChRs (C_2), $\alpha4*$ nAChRs (C_3) and $\alpha6*$ nAChRs (C_4). Linear fits (red line) with 95% confidence intervals (dotted red lines) were applied using Graphpad Prism software. Nicotine correlations used 7 male and 8 female $\alpha4$-mCherry$\alpha6$-GFP mice and the saline correlations used 5 $\alpha4$-mCherry$\alpha6$-GFP mice (3 males and 2 females). For each mouse, 36–71 neurons were imaged.

Figure Contributions: Austin T. Akers, Zachary J. Baumgard, and Brandon J. Henderson performed the experiments and analyzed the data.

behavior. These correlative data may imply that the upregulation of $\alpha4*$ and $\alpha4\alpha6*$ nAChRs may underlie nicotine reward-related behavior, at least in the context of CPP assays.

Upregulation of $\alpha4\beta2*$ nAChRs on GABA neurons of the VTA and SNr

The upregulation of $\alpha4\beta2*$ nAChRs on GABA neurons may play an important role in nicotine's rewarding effect in the mesolimbic circuit (Mansvelder et al., 2002; Nashmi et al., 2007). Nashmi et al. (2007) showed that $\alpha4*$ nAChRs exhibit a greater degree of upregulation on GABA neurons (VTA and SNr) than they do on DA neurons. In VTA GABA neurons, we observed a significant, 3.4-fold increase in $\alpha4$-mCherry RID ($p = 0.01$; Fig. 4A1, A2). In male and female mice, we observed a significant correlation between $\alpha4*$ nAChR upregulation in VTA GABA neurons and nicotine reward-related behavior (males, $R^2 = 0.55$, $F_{(1,6)} = 7.39$, and $p = 0.04$; and females, $R^2 = 0.56$, $F_{(1,6)} = 6.5$, $p = 0.05$; Fig. 4A3,A4). Similar to the case of $\alpha6*$ nAChR upregulation in male mice, we note that the slope of this correlation is relatively flat.

SNr GABA neurons in mice from the nicotine CPP group exhibited a 2.4-fold increase in $\alpha4$-mCherry RID that was significant compared with saline-treated mice ($p = 0.02$; Fig. 4B1,B2). While this increase in $\alpha4*$ nAChRs is robust, we observed no correlation between $\alpha4*$ nAChR upregulation in SNr GABA neurons and nicotine reward-related behavior in either male or female mice (Fig. 4B3). These data show that concentrations of nicotine sufficient to evoke reward-related behavior upregulate $\alpha4\beta2$ nAChRs on GABA neurons in the VTA and SNr. Given the absence of a strong correlation between upregulation and nicotine reward-related behavior, these data also suggest that VTA DA neurons may be more critical for the initiation of nicotine reward. However, this finding needs to be followed-up with functional experiments to examine changes in neurophysiology (see below).

We also investigated how nicotine reward-related behavior is linked to nAChR upregulation in the dentate gyrus (ventral hippocampus; bregma, -3.1; Fig. 4C1,C2). We observed no significant upregulation in the dentate gyrus of the mice that were part of the nicotine CPP cohort. In fact, we observed a significant decrease in $\alpha4*$ nAChR density ($p = 0.047$; Fig. 4D1). Previous investigations did detect upregulation in the dentate gyrus (Nashmi et al., 2007); but this was with a persistent, high dose of nicotine (2 mg/kg/h via osmotic minipumps for 10 d). Thus, while upregulation is noted with $\alpha4*$ nAChRs in the dentate gyrus with high doses of nicotine, we did not notice upregulation with doses used (0.5 mg/kg injections) to produce reward-related behavior.

Changes in VTA pDA and putative GABA (pGABA) neuron firing frequency correlates to reward-related behavior

While upregulation may indicate changes in nAChR number on neurons, we acknowledge that our confocal methods do not directly indicate whether the upregulation

is indicative of increases in intracellular or plasma membrane bound nAChRs. Thus, we used brain-slice electrophysiology to determine whether changes in VTA pDA and pGABA neuron function are linked to reward-related behavior. Nicotine has been observed to decrease the baseline firing frequency of VTA DA neurons and increase the firing frequency of VTA and SNr GABA neurons (Mansvelder et al., 2002; Nashmi et al., 2007). We used a separate cohort of mice assigned to saline or nicotine in CPP assays (Fig. 5C). Similar to results described above, we noted a significant difference between saline-treated and nicotine-treated mice in our CPP assay ($p = 0.02$). Similar to microscopy assays, at the end of CPP, mouse brains were extracted but here were used for brain-slice electrophysiology assays. Similar to microscopy assays, we used $\alpha6$-GFP fluorescence to identify pDA neurons in the $_L$VTA (Fig. 5A,B1,B2). Using cell-attached configurations we examined baseline firing frequency of VTA pDA neurons (Fig. 5D). Here, we observed that nicotine-treated mice exhibited a significant decrease in baseline firing of VTA pDA neurons ($p = 0.009$; Fig. 5E) that matches previous investigations (Nashmi et al., 2007; Xiao et al., 2009). Next, we correlated the VTA pDA neuron firing frequency of individual nicotine-treated mice (mean of $\geq$3 neurons per mouse) to its respective CPP score (Fig. 5F). We observed a significant inverse-correlation between firing frequency of VTA pDA neurons and nicotine reward-related behavior ($R^2 = 0.65$, $F_{(1,6)} = 11.2$, $p = 0.016$).

Using these same mice, we examined the firing frequency of VTA pGABA neurons (Fig. 6A,B1,B2). Similar to previous reports, we noted a significant increase in the baseline firing frequency of VTA pGABA neurons in mice assigned to the nicotine CPP cohort (Fig. 6D). Despite observing no significant correlation between nicotine reward-related behavior and $\alpha4\beta2$ nAChR upregulation in VTA GABA neurons (or SNr GABA neurons), we did observe a significant correlation between nicotine reward-related behavior and VTA pGABA neuron firing frequency ($R^2 = 0.77$, $F_{(1,16)} = 20.3$, $p = 0.004$; Fig. 6E).

Discussion

It is important to note that nAChRs on VTA DA neurons would be functionally activated as our data (300 and 500 nM nicotine; Fig. 2) and previous investigations (300 nM; Liu et al., 2012; Engle et al., 2013) show that nicotine concentrations that match those present in CPP assays are sufficient to evoke inward currents in VTA DA neurons. These previous reports also stress that activation with this low concentration of nicotine only activates nAChRs that contain $\alpha4$ and $\alpha6$ subunits. In line with these previous studies, we noted a significant link between nicotine reward-related behavior and $\alpha4\alpha6*$ nAChRs, $\alpha4$(non-$\alpha6$)* nAChRs, but not $\alpha6$(non-$\alpha4$)* nAChRs, in the $_L$VTA. We observed no relationship between $\alpha4*$ nAChR upregulation in the SNr to nicotine reward-related behavior. This finding matches a previous investigation by Pons et al. (2008) that showed nicotine self-administration in mice depends on $\alpha4*$, $\alpha6*$, and $\beta2*$ nAChRs in the VTA but not in the substantia nigra.

One limitation of the current study is that we only observed a single time point (the final CPP test day). The
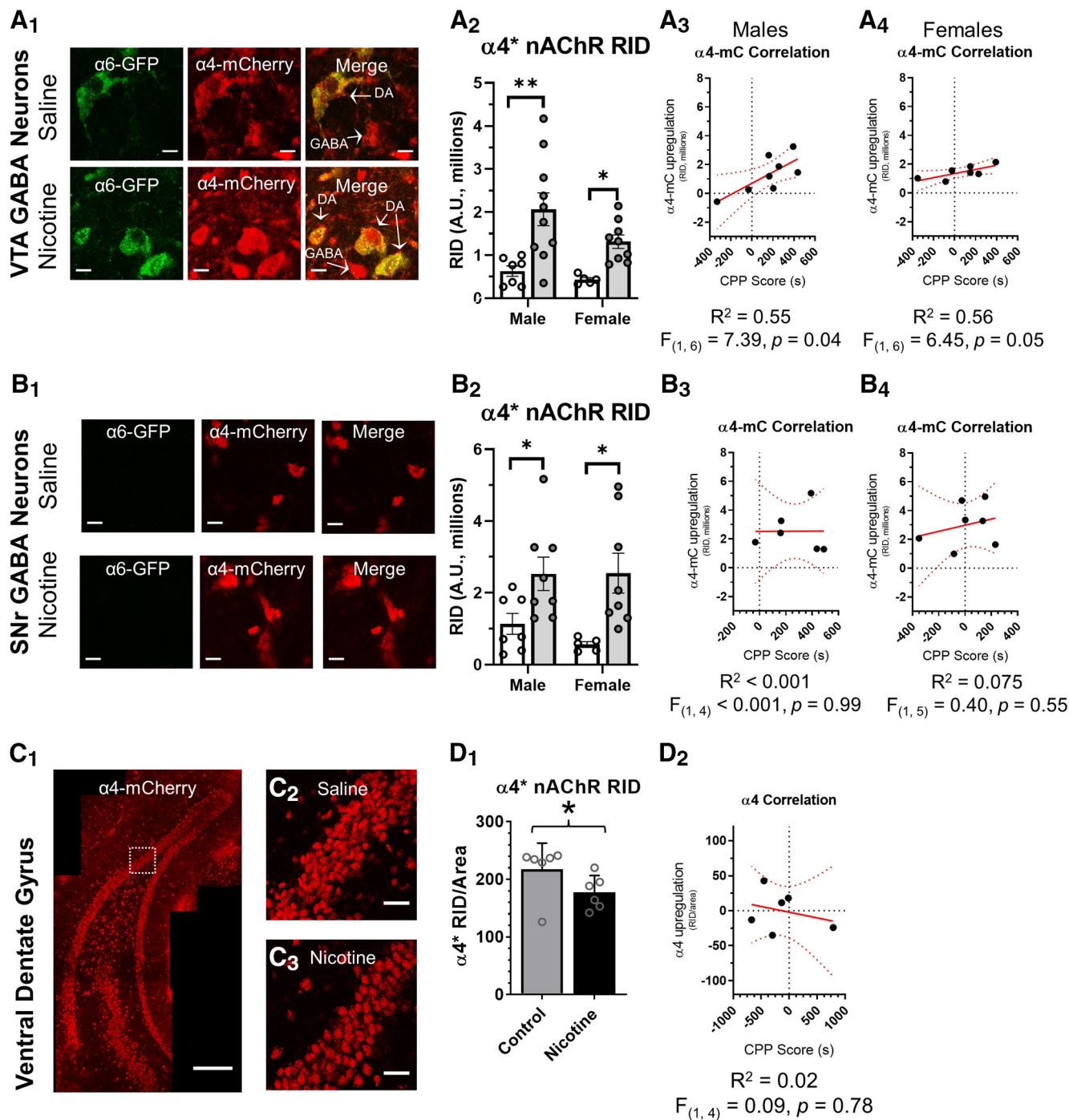
Figure 4. Upregulation of $\alpha4*$ nAChRs on SNr and VTA putative GABAergic neurons may not correlate with nicotine reward-related behavior. **A_1, B_1,** and **C_1,** Representative images of neurons in the $_L$VTA (**A_1**), SNr (**B_1**), or dentate gyrus (**C**) in a $\alpha4$-mCherry$\alpha6$-GFP brain slice. Scale bar, 10 μm (**A_1** and **B_1**), 250 μm (**C_1**), and 25 μm (**C_2, C_3**). **A_2, B_2,** RID of saline- and nicotine-treated mice from CPP assays for SNr GABA neurons or VTA GABA neurons. In **A_2** and **B_2** the n of individual male and female mice are indicated by individual dots. In nicotine-treated mice, changes in nAChR RID was correlated to CPP score for $\alpha4*$ nAChRs in SNr GABA neurons or VTA GABA neurons. In **A_3, A_4, B_3,** and **B_4** the n of individual male and female mice are indicated by individual dots. **D_1,** RID/area of saline- and nicotine-treated mice from CPP assays for dentate gyrus ($n = 6$, 3 male and 3 female). **D_2,** Changes in nAChR RID/area was correlated to CPP score for $\alpha4*$ nAChRs in the dentate gyrus. Linear fits (red line) with 95% confidence intervals (dotted red lines) were applied using Graphpad Prism software. Data is Mean $\pm$ SEM; $*p = 0.05$, $**p = 0.01$; unpaired, two-tailed t test.
Figure Contribution: Austin T. Akers, Zachary J. Baumgard, Skylar Y. Cooper, Alicia J. Avelar, and Brandon J. Henderson performed the experiments and analyzed the data.
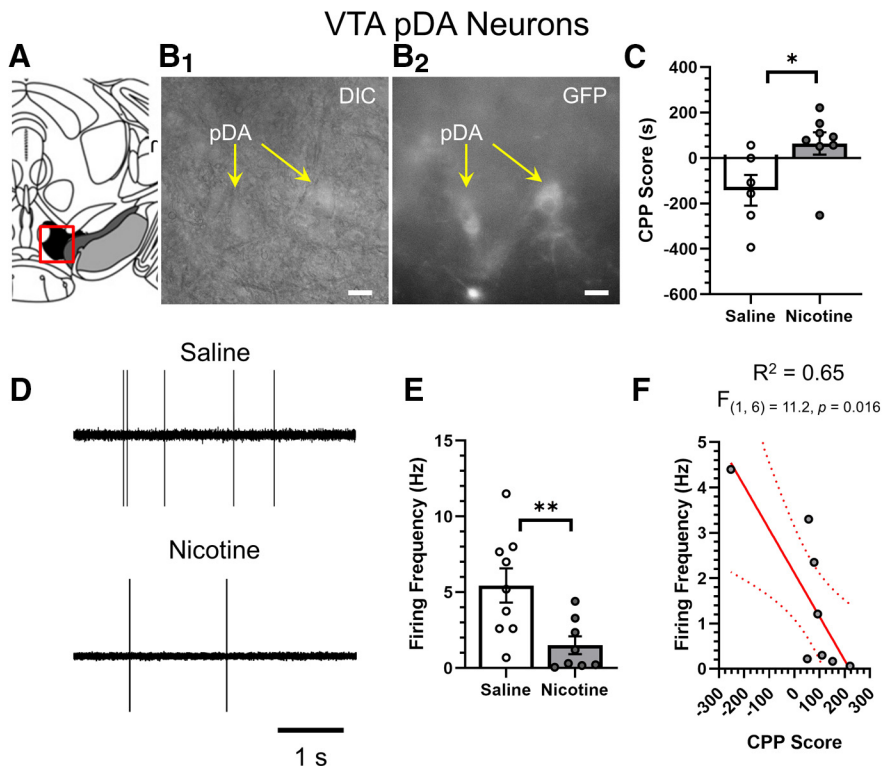
VTA pDA Neurons

Figure 5. Decreases in VTA pDA neuron firing frequency correlates with reward-related behavior. **A**, Schematic of target neurons within the ₗVTA (target bregma, −3.1). **B₁**, **B₂**, Representative images of VTA pDA neurons in DIC (**B₁**) and GFP (**B₂**) imaging modes. Scale bar: 20 μm. Mice used in CPP assays (**C**) were used to measure firing frequency of pDA neurons in the VTA (**D, E**). **D**, Representative cell-attached recordings of VTA pDA neuron baseline firing frequency. **E**, Mean VTA pDA neuron firing frequency in mice treated with saline or nicotine in CPP assays. Data are mean ± SEM, dots represent data from individual mice ($n = 8–9$ per condition). **F**, Reward-related behavior (CPP Score) was correlated to baseline firing frequency of ₗVTA pDA neurons; *$p < 0.05$, **$p < 0.01$; unpaired t test. Exact p values are given in text.

Figure Contributions: Brandon J. Henderson performed the experiments and analyzed the data.

problem this poses is that our analysis of upregulation and neuronal firing frequency captures the target nAChRs in a state that is free of nicotine for ~24 h. As a result, even in this case where we observed nAChR upregulation and changes in firing frequency in our assays, we ca not adequately assess how nicotine-induced activation of the nAChRs connects to our observed reward-related behavior. Furthermore, our behavioral assay (CPP) is a non-contingent assay and while it provides information regarding nicotine-related reward, it does not provide insight into reinforcement or the impact of long-term nicotine exposure. One manner to improve on this would be to use a contingent drug delivery assay (intravenous or vapor self-administration). With these assays we would be able to extract the brains immediately after operant responding so that we can capture the behavioral endpoint and the brain samples that are still saturated with nicotine. Thus, we could examine changes to nAChRs while nicotine is present and use a model that more closely matches smoking-related behaviors. These assays (vapor self-administration) are currently being pursued but are only at their early stages.

Previous reports show that nicotine robustly upregulates high-sensitivity $\alpha4\beta2$ nAChRs on SNr and VTA GABAergic neurons (Nashmi et al., 2007; Xiao et al., 2009), and we have reproduced that here (Fig. 4). Interestingly, our data show a link between $\alpha4*$ nAChR upregulation on VTA pGABA neurons and nicotine reward-related behavior but no correlation between upregulation of $\alpha4*$ nAChRs on SNr pGABA neurons and reward-related behavior. For $\alpha4\beta2$ nAChR upregulation on VTA GABA neurons, the R^2 values of 0.55 and 0.56 (males and females, respectively) may indicate their upregulation is less sensitive when compared with what we observed on pDA neurons. Here, we must also take into consideration that pDA neurons have a multitude of nAChR subtypes that assemble in multiple possible stoichiometries [$\alpha4\beta2$ ($\alpha4_{(3)}\beta2_{(2)}$ and $\alpha4_{(2)}\beta2_{(3)}$), $\alpha4\alpha6\beta2$ ($\alpha4_{(1)}\alpha6_{(1)}\beta2_{(3)}$, $\alpha4_{(2)}\alpha6_{(1)}\beta2_{(2)}$, $\alpha4_{(1)}\alpha6_{(2)}\beta2_{(2)}$, $\alpha4_{(1)}\alpha6_{(1)}\beta2_{(2)}\beta3_{(1)}$, and potentially others), and $\alpha6\beta2*$ (mostly $\alpha6_{(2)}\beta2_{(2)}\beta3_{(1)}$)]. Thus, we must acknowledge that changes in RID of nAChR subunits may also be the result of a net change in stoichiometry. This is another weakness of our methods as we cannot distinguish between nAChRs that reside on the plasma membrane from those that are intracellular. Additionally, we can detect changes in stoichiometry but not define specific stoichiometries. The former problem (plasma membrane changes) is partially reconciled by our electrophysiology assays (discussed below) but the latter can
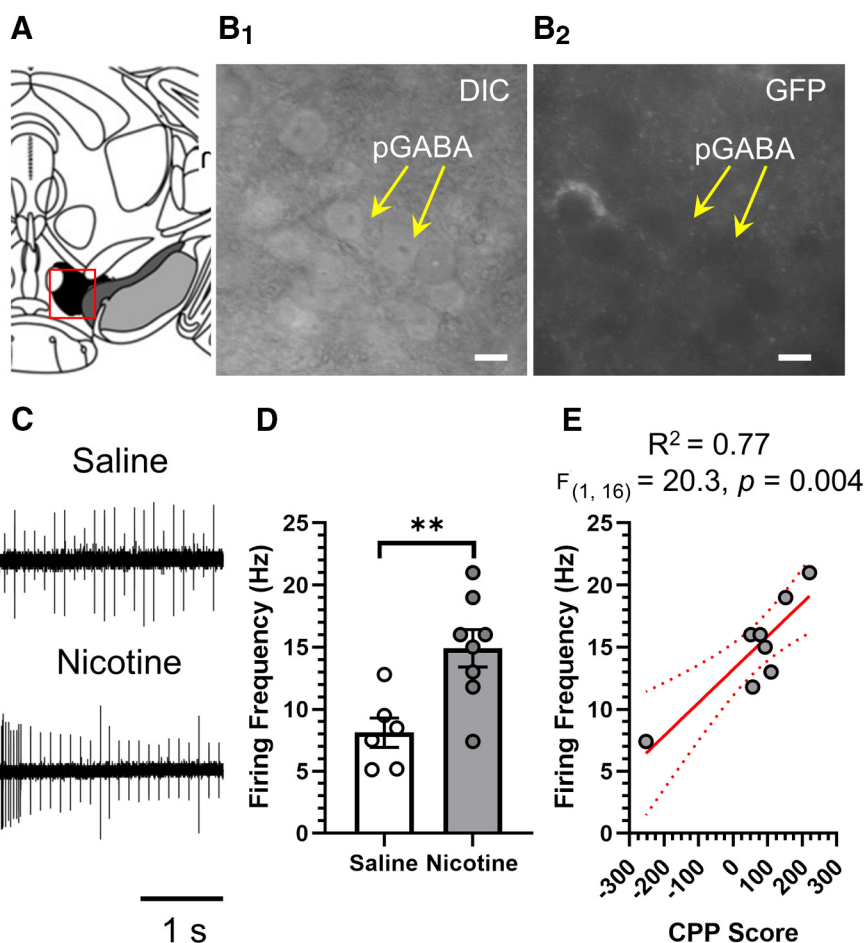
VTA pGABA Neurons

Figure 6. Increase in VTA pGABA neuron firing frequency correlates with reward-related behavior. ***A***, Schematic of target pGABA neurons within the $_L$VTA (target bregma, −3.1). ***B$_1$***, ***B$_2$***, Representative images of VTA pGABA neurons in DIC (***B$_1$***) and GFP (***B$_2$***) imaging modes. Scale bar: 20 μm. ***C***, Representative cell-attached recordings of VTA pGABA neuron baseline firing frequency from mice assigned to saline or 0.5 mg/kg nicotine CPP cohorts. ***D***, Mean VTA pGABA neuron firing frequency in mice treated with saline or nicotine in CPP assays. Data are mean ± SEM ***E***, Reward-related behavior (CPP Score) were correlated to baseline firing frequency of VTA pGABA neurons; ∗∗$p < 0.01$ with; unpaired t test. Exact p values are given in text.
Figure Contributions: Brandon J. Henderson performed the experiments and analyzed the data.

now be addressed using newly developed single-molecule microscopy assays (Fu et al., 2019).

Our electrophysiological methods detected a correlation between VTA pGABA neurons and reward-related behavior that is greater than the correlation between VTA pDA neuron firing and reward-related behavior. One conclusion for this is that our electrophysiological methods are more sensitive than that of our microscopy assays. While this is likely true, the caveat is that brain-slice electrophysiology is lower throughput as we can examine 4–10 neurons per mouse, while there are hundreds of neurons in each brain region that could be measured using microscopy. Consequently, the electrophysiological methods may be a more accurate determination of changes in neuronal populations in relation to reward-related behavior.

Following recent investigations into VTA DA and GABA neurons (Grieder et al., 2019), a second conclusion is that

there is a distinct difference in the role that DA and GABA systems play within the VTA in nicotine reward. The work by Grieder et al. (2019) revealed that VTA DA neurons mediate aversion while VTA GABA neurons mediate reward to nicotine. This finding also agrees with another previous report that revealed the selective upregulation of $\alpha4\beta2*$ nAChRs on VTA GABA neurons was sufficient to produce CPP in mice and increased sensitivity to nicotine reward (Ngolab et al., 2015). Our observations of an inverse-correlation between VTA pDA neuron firing and nicotine reward but a positive correlation between VTA pGABA neuron firing and nicotine reward may support these previous conclusions. One way to address distinction between aversive and rewarding stimuli within the VTA with our current methodology would be to repeat these microscopy and electrophysiology assays but with a conditioned place aversion paradigm using a higher, aversive dose of nicotine.

While this study focuses on DA and GABA neurons of the midbrain, there are other cell types and brain regions that are critical to nicotine reward and reinforcement. Accordingly, our understanding of how changes in nAChR upregulation and function directly link to reward (or reinforcement) is still in the beginning stages and have yet to examine the recently defined local nicotine-related glutamatergic inputs (Yan et al., 2018, 2019) or the aversive stimuli that originate from the habenula and interpeduncular nuclei (Fowler et al., 2011; Fowler and Kenny, 2012). The methods of this study should be applied to several additional behavioral aspects of chronic nicotine, namely nicotine self-administration. At present, our data show that the upregulation of $\alpha 4*$ and $\alpha 4 \alpha 6*$ nAChRs in VTA neurons is tied to nicotine reward-related behavior.

References

Avelar AJ, Akers AT, Baumgard ZJ, Cooper SY, Casinelli GP, Henderson BJ (2019) Why flavored vape products may be attractive: green apple tobacco flavor elicits reward-related behavior, upregulates nAChRs on VTA dopamine neurons, and alters midbrain dopamine and GABA neuron function. Neuropharmacology 158:107729.

Cooper SY, Akers AT, Henderson BJ (2020) Green apple e-cigarette flavorant farnesene triggers reward-related behavior by promoting high-sensitivity nAChRs in the ventral tegmental area. eNeuro 7:ENEURO.0172-20.2020.

Engle SE, Shih PY, McIntosh JM, Drenan RM (2013) $\alpha 4 \alpha 6 \beta 2*$ nicotinic acetylcholine receptor activation on ventral tegmental area dopamine neurons is sufficient to stimulate a depolarizing conductance and enhance surface AMPA receptor function. Mol Pharmacol 84:393–406.

Fowler CD, Kenny PJ (2012) Habenular signaling in nicotine reinforcement. Neuropsychopharmacology 37:306–307.

Fowler CD, Lu Q, Johnson PM, Marks MJ, Kenny PJ (2011) Habenular $\alpha 5$ nicotinic receptor subunit signalling controls nicotine intake. Nature 471:597–601.

Fu X, Moonschi FH, Fox-Loe AM, Snell AA, Hopkins DM, Avelar AJ, Henderson BJ, Pauly JR, Richards CI (2019) Brain region specific single-molecule fluorescence imaging. Anal Chem 91:10125–10131.

Grieder TE, Besson M, Maal-Bared G, Pons S, Maskos U, van der Kooy D (2019) $\beta 2*$ nAChRs on VTA dopamine and GABA neurons separately mediate nicotine aversion and reward. Proc Natl Acad Sci USA 116:25968–25973.

Henderson BJ, Srinivasan R, Nichols WA, Dilworth CN, Gutierrez DF, Mackey ED, McKinney S, Drenan RM, Richards CI, Lester HA (2014) Nicotine exploits a COPI-mediated process for chaperone-mediated up-regulation of its receptors. J Gen Physiol 143:51–66.

Henderson BJ, Wall T, Henley BM, Kim CH, Nichols WA, Moaddel R, Xiao C, Lester HA (2016) Menthol alone upregulates midbrain nAChRs, alters nAChR sybtype stoichiometry, alters dopamine neuron firing frequency, and prevents nicotine reward. J Neurosci 36:2957–2974.

Henderson BJ, Wall TR, Henley BM, Kim CH, McKinney S, Lester HA (2017) Menthol enhances nicotine reward-related behavior by potentiating nicotine-induced changes in nAChR function, nAChR upregulation, and DA neuron excitability. Neuropsychopharm 24:2285–2291.

Jasinska AJ, Zorick T, Brody AL, Stein EA (2014) Dual role of nicotine in addiction and cognition: a review of neuroimaging studies in humans. Neuropharmacology 84:111–122.

Kuryatov A, Lindstrom J (2011) Expression of functional human $\alpha 6 \beta 2 \beta 3$ acetylcholine receptors in Xenopus laevis oocytes achieved through subunit chimeras and concatamers. Mol Pharmacol 79:126–140.

Kuryatov A, Luo J, Cooper J, Lindstrom J (2005) Nicotine acts as a pharmacological chaperone to up-regulate human alpha4beta2 acetylcholine receptors. Mol Pharmacol 68:1839–1851.

Li L, Jia K, Zhou X, McCallum SE, Hough LB, Ding X (2013) Impact of nicotine metabolism on nicotine's pharmacological effects and behavioral responses: insights from a Cyp2a(4/5)bgs-null mouse. J Pharmacol Exp Ther 347:746–754.

Liu L, Zhao-Shea R, McIntosh JM, Gardner PD, Tapper AR (2012) Nicotine persistently activates ventral tegmental area dopaminergic neurons via nicotinic acetylcholine receptors containing $\alpha 4$ and $\alpha 6$ subunits. Mol Pharmacol 81:541–548.

Mackey ED, Engle SE, Kim MR, O'Neill HC, Wageman CR, Patzlaff NE, Wang Y, Grady SR, McIntosh JM, Marks MJ, Lester HA, Drenan RM (2012) $\alpha 6*$ nicotinic acetylcholine receptor expression and function in a visual salience circuit. J Neurosci 32:10226–10237.

Mansvelder HD, Keath JR, McGehee DS (2002) Synaptic mechanisms underlie nicotine-induced excitability of brain reward areas. Neuron 33:905–919.

Margolis EB, Lock H, Hjelmstad GO, Fields HL (2006) The ventral tegmental area revisited: is there an electrophysiological marker for dopaminergic neurons? J Physiol 577:907–924.

Marks MJ, Burch JB, Collins AC (1983) Effects of chronic nicotine infusion on tolerance development and nicotinic receptors. J Pharmacol Exp Ther 226:817–825.

Matta SG, Balfour DJ, Benowitz NL, Boyd RT, Buccafusco JJ, Caggiula AR, Craig CR, Collins AC, Damaj MI, Donny EC, Gardiner PS, Grady SR, Heberlein U, Leonard SS, Levin ED, Lukas RJ, Markou A, Marks MJ, McCallum SE, Parameswaran N, et al. (2007) Guidelines on nicotine dose selection for in vivo research. Psychopharmacology (Berl) 190:269–319.

Nashmi R, Xiao C, Deshpande P, McKinney S, Grady SR, Whiteaker P, Huang Q, McClure-Begley T, Lindstrom JM, Labarca C, Collins AC, Marks MJ, Lester HA (2007) Chronic nicotine cell specifically upregulates functional $\alpha 4*$ nicotinic receptors: basis for both tolerance in midbrain and enhanced long-term potentiation in perforant path. J Neurosci 27:8202–8218.

National Center for Chronic Disease Prevention and Health Promotion (US) Office on Smoking and Health (2014) The health consequences of smoking - 50 years of progress: a report of the surgeon general. Atlanta: Centers for Disease Control and Prevention.

Ngolab J, Liu L, Zhao-Shea R, Gao G, Gardner PD, Tapper AR (2015) Functional upregulation of $\alpha 4*$ nicotinic acetylcholine receptors in VTA GABAergic neurons increases sensitivity to nicotine reward. J Neurosci 35:8570–8578.

Pons S, Fattore L, Cossu G, Tolu S, Porcu E, McIntosh JM, Changeux JP, Maskos U, Fratta W (2008) Crucial role of $\alpha 4$ and $\alpha 6$ nicotinic acetylcholine receptor subunits from ventral tegmental area in systemic nicotine self-administration. J Neurosci 28:12318–12327.

Sanjakdar SS, Maldoon PP, Marks MJ, Brunzell DH, Maskos U, McIntosh JM, Bowers MS, Damaj MI (2015) Differential roles of $\alpha 6 \beta 2*$ and $\alpha 4 \beta 2*$ neuronal nicotinic receptors in nicotine- and cocaine-conditioned reward in mice. Neuropsychopharmacology 40:350–360.

Srinivasan R, Henley BM, Henderson BJ, Indersmitten T, Cohen BN, Kim CH, McKinney s, Deshpande P, Xiao C, Lester HA (2016) Smoking-relevant nicotine concentration attenuates the unfolded protein response in dopaminergic neurons. J Neurosci 36:65–79.

Tapper AR, McKinney SL, Nashmi R, Schwarz J, Deshpande P, Labarca C, Whiteaker P, Marks MJ, Collins AC, Lester HA (2004) Nicotine activation of alpha4* receptors: sufficient for reward, tolerance and sensitization. Science 306:1029–1032.

Vallejo YF, Buisson B, Bertrand D, Green WN (2005) Chronic nicotine exposure upregulates nicotinic receptors by a novel mechanism. J Neurosci 25:5563–5572.

World Health Organization (2011) WHO report on the global tobacco epidemic. Geneva: World Health Organization.

Xiao C, Nashmi R, McKinney S, Cai H, McIntosh JM, Lester HA (2009) Chronic nicotine selectively enhances alpha4beta2∗ nicotinic acetylcholine receptors in the nigrostriatal dopamine pathway. J Neurosci 29:12428–12439.

Yan Y, Peng C, Arvin MC, Jin XT, Kim VJ, Ramsey MD, Wang Y, Banala S, Wokosin DL, McIntosh JM, Lavis LD, Drenan RM (2018) Nicotinic cholinergic receptors in VTA glutamate neurons modulate excitatory transmission. Cell Rep 23:2236–2244.

Yan Y, Beckley NA, Kim VJ, Drenan RM (2019) Differential nicotinic modulation of glutamatergic and GABAergic VTA microcircuits. eNeuro 6.

Yang K, Buhlman L, Khan GM, Nichols RA, Jin G, McIntosh JM, Whiteaker P, Lukas RJ, Wu J (2011) Functional nicotinic acetylcholine receptors containing α6 subunits are on GABAergic neuronal boutons adherent to ventral tegmental area dopamine neurons. J Neurosci 31:2537–2548.